J. of Supercritical Fluids 57 (2011) 137–142

Contents lists available at ScienceDirect

The Journal of Supercritical Fluids

journal homepage: www.elsevier.com/locate/supflu

Reaction of hydrous inorganic metal salts in CO_2 expanded ethanol: Fabrication of nanostructured materials via supercritical technology

Jun Ming[a,b,c], Chaoyong Wu[a,b,c], Haiyang Cheng[a,b], Yancun Yu[a,b], Fengyu Zhao[a,b,*]

[a] State Key Laboratory of Electroanalytical Chemistry, Changchun Institute of Applied Chemistry, Chinese Academy of Sciences, Changchun 130022, PR China
[b] Laboratory of Green Chemistry and Process, Changchun Institute of Applied Chemistry, Chinese Academy of Sciences, Changchun 130022, PR China
[c] University of the Chinese Academy of Sciences, Beijing 100049, PR China

ARTICLE INFO

Article history:
Received 18 December 2010
Received in revised form 6 March 2011
Accepted 7 March 2011

Keywords:
CO_2-expanded solution
Reaction behavior
Metal salt
Nanostructured materials

ABSTRACT

The fabrication of nanostructured materials from hydrous inorganic metal salt processed in supercritical CO_2 ($scCO_2$) expanded liquids has advantages to obtain good results. However, the behavior of the inorganic salts and the detailed reaction mechanism are still unknown up to now. In this work, the actual behavior of hydrous inorganic metal salts in CO_2 expanded ethanol at the temperature of 50–200 °C, including the phase behavior, deposition mechanism, reaction rate and the effect of templates on the deposition were systematically investigated by using XRD, FTIR, CHN-analysis, TGA, ICP-AES. A series of experimental parameters such as CO_2 flow rate, expand procedure, reaction temperature and time have been discussed, as well as the roles of CO_2 and H_2O (often originated from salts and/or solvent but always neglected) were studied in this contribution. Significantly, a coordination–decomposition (C–D) was proved to be the converting mechanism for the precipitation of the hydrous inorganic metal salts, rather than the fuzzy decomposition.

1. Introduction

Supercritical carbon dioxide ($scCO_2$) has advantages in the deposition of metal (oxides) onto a wide range of porous substrates through the supercritical fluid deposition method, because the low viscosity and high diffusivity of $scCO_2$ relative to liquids, together with its low surface tension could largely mitigate the mass transfer limitations and then facilitate the infiltration of precursors in complex geometries. During the past few decades, numerous organometallic compounds, including dimethyl(1,5-cyclooctadiene)platinum(II) [$CODPtMe_2$] [1–4], 2-methylallyl(cyclopentadienyl)palladium(II) [$CpPd(\pi\text{-}C_4H_7)$] [5,6], CpNi/CpCo [7], bis(2,2,6,6-tetramethyl-3,5-heptanedionate) copper(II) [$Cu(tmhd)_2$] [8,9], $Ru(COD)(tmhd)_2$ [10,11], (1,5-cyclooctadiene)(1,1,1,5,5,5-hexafluoroacetylacetonate)silver(I) Ag(hfac)COD [12], dimethyl(acetylacetonate)gold(III) [$(acac)Au(CH_3)_2$] [13], have been studied as precursors to deposit Pt, Pd, Cu, Ni, Co, Ru, Ag and Au films and nanoparticles on inorganic or organic substrates [14,15]. Moreover, a series of metal alkoxides (metal = Si, Ti, Zr, Al, etc.) has been also hydrolyzed in $scCO_2$ for the fabrication of metal oxides with diverse structures, such as porous aerogel [16], nanoparticle and fiber [17,18], or the deposition of metal oxides on a wide variety of templates, including active carbon [19], fiber [20], etched wafer [21], biological materials [22], giving rise to precise inverse-template structured metal oxides. To date, the wide use of organometallic precursors was determined by their specific relative high solubility in $scCO_2$ [23]. However, the organometallic compounds are always expensive, difficult to store and manipulate, and harmful compared with hydrous inorganic metal salts. Therefore, there is a strong tendency to design a green strategy that uses hydrous inorganic metal salts instead of organometallic ones as precursors for the deposition and preparation of nanostructured materials, even though their solubility is limited in $scCO_2$.

Recently, the solubility problem of the hydrous inorganic metal salt has been overcome through introducing the co-assistant solvent such as ethanol and methanol into the system, to form a $scCO_2$ expanded fluid. Han et al. [24–26] demonstrated that $scCO_2$ expanded ethanol can disperse hydrous metal nitrates inside and outside of carbon nanotubes (CNTs) and form a uniform oxide coating on tubes via in situ "decomposition" of precursors. A series of multi-functional composite materials, such as Al_2O_3/CNTs [24], CeO_2/CNTs [25] and ZrO_2/CNTs [26] etc. have been prepared in $scCO_2$ expanded ethanol, which are difficult to obtain in pure ethanol. The unique physicochemical properties of the expanded fluid, such as low viscosity and surface tension and high diffusivity are responsible for the formation of the uniform coating of oxides. However, further study should be required on the role of

* Corresponding author at: Changchun Institute of Applied Chemistry, State Key Laboratory of Electroanalytical Chemistry, 5625 Renmin Street, Changchun, Jilin 130022, China. Tel.: +86 0431 85262410; fax: +86 431 85262410.
E-mail address: zhaofy@ciac.jl.cn (F. Zhao).

0896-8446/$ – see front matter © 2011 Elsevier B.V. All rights reserved.
doi:10.1016/j.supflu.2011.03.003

CO_2 molecules and the features of deposition reactions in $scCO_2$ expanded solution. In this work, we investigate the reaction behavior of hydrous inorganic metal salts in $scCO_2$ expanded ethanol, including the phase behavior, deposition mechanism, reaction rate and the effect of templates on the deposition. In addition, a series of experimental parameters such as CO_2 flow rate, expand procedure, reaction temperature and time have been discussed, as well as the roles of CO_2 and H_2O (often originated from salts and/or solvent but always neglected) were studied.

2. Experimental

2.1. Materials

The analytical chemical reagents of $Ni(NO_3)_2{\cdot}6H_2O$, $Fe(NO_3)_3{\cdot}9H_2O$, $Co(NO_3)_2{\cdot}6H_2O$ $Zn(NO_3)_2{\cdot}6H_2O$, $Cu(NO_3)_2{\cdot}3H_2O$, $Cr(NO_3)_3{\cdot}9H_2O$, $Nd(NO_3)_3{\cdot}6H_2O$, $SnCl_2{\cdot}4H_2O$, $MnCl_2{\cdot}4H_2O$ and C_2H_5OH were purchased from Sinopharm Chemical Reagent Beijing Co. Ltd., and $PdCl_2$ was purchased from Aldrich. All the chemicals were used directly without further purification. The templates of carbon colloids and silica nanoparticles were synthesized through hydrothermal method [27] and Stöber process [28], respectively.

2.2. Phase behavior

A volume of 16 ml ethanol solution of hydrous inorganic metal salt with a given concentration (0–0.2 M) was charged in a viewable autoclave (80 ml), and then introduced CO_2 with a flow rate of 7 ml/min at the temperature of 80 °C for $Fe(NO_3)_3{\cdot}9H_2O$, 100 °C for $Cu(NO_3)_2{\cdot}3H_2O$, and 150 °C for others (e.g., $Co(NO_3)_2{\cdot}6H_2O$, $Ni(NO_3)_2{\cdot}6H_2O$) to expand the solution, until the solution was expanded to fill up the autoclave with homogeneous fluid. After the fluid was stable for a few minutes, increased the temperature to 200 °C with a heating rate of 3 °C/min and reacted at that temperature for 2 h, under which the soluble inorganic metal salts was completely converted into solid compounds and precipitated from the fluid.

2.3. Characterization

Crystallographic information was investigated by XRD patterns with a Brucker D8 GADDS diffractometer using Co Kα radiation (1.79 Å), and the crystallite size was calculated using Scherrer's equation. The existence of CO_3^{2-} and/or NO_3^- in resultant solid-compounds was confirmed by CHN-analysis (VarioEL CHN). The content of water and hydroxyl groups were confirmed by Thermogravimetric Analysis (TGA) curves (Pyris Diamond TG/DTA) in the temperature range of 40–550 °C with a heating rate of 10 °C/min under N_2 atmosphere. The chemical bond information of free NO_3^- (D_{3h} symmetry), M–O, M–OH, M–OCO_2/(M–OCOO–) and M–ONO_2/(M–ONOO–) (C_{2v} symmetry) were confirmed by Fourier transform infrared spectroscopy (FTIR) that recorded with Bruker Vertex 70 in the frequency range of 4000–450 cm^{-1}. The content of metallic ions in residual solution was measured by inductively coupled plasma atomic emission spectrometer (ICP-AES) (Thermo Scientific iCAP 6000 Series).

3. Results and discussion

3.1. Factors affecting phase behavior

Although the $scCO_2$ has been widely used in the fabrication of nanostructured materials through forming the expanded ethanol solution of metal nitrates [24–26], the experimental parameters and the actual behavior of metal nitrates in the system have been not discussed in detail. Experimental parameters affect on the formation of expanded homogeneous fluid and the deposition of hydrous inorganic metal salts, and this point needs examination.

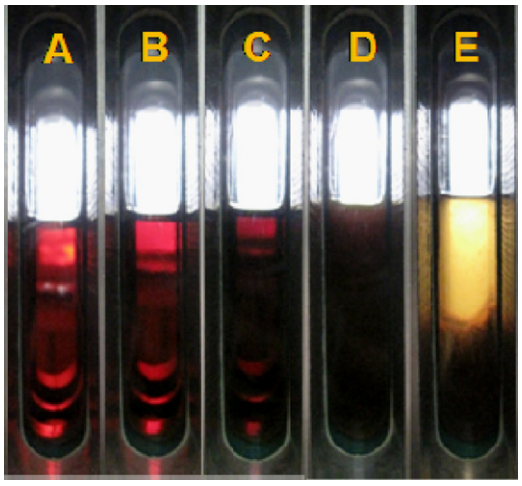

Fig. 1. Phase behavior of $Fe(NO_3)_3{\cdot}9H_2O$ (0.05 M) under stirring (A–D) in a sealed autoclave at different temperatures without CO_2 expansion. (A) 50 °C, (B) 80 °C, (C) 100 °C, (D) 120 °C. (E) the static phase of (D).

Firstly, a suitable temperature (T) is an essential factor for ensuring the reaction of precursors occurs in the expanded fluid, because the hydrous inorganic metal salt could deposit before the expansion process if the temperature is too high. For example, $Fe(NO_3)_3{\cdot}9H_2O$ (0.05 M) could form the precipitate in ethanol within 5 min at 120 °C (Fig. 1), therefore a temperature around 80–100 °C was practicable for $Fe(NO_3)_3{\cdot}9H_2O$ to form a homogenous CO_2 expanded ethanol solution for that $Fe(NO_3)_3{\cdot}9H_2O$ was stable in ethanol at these temperatures. While other nitrates such as cobalt, nickel and chromium nitrates could be stable at 150 °C in ethanol, at which it is reasonable to expand. Fig. 2 shows that the ethanol solution of $Ni(NO_3)_2{\cdot}6H_2O$ (0.02 M) was well expanded to form a homogeneous fluid filled up of autoclave under the pressure of 14.1 MPa without any reaction. Generally, selecting a relative high temperature (100–150 °C) to expand is good for reducing the final pressure of the system, particularly for that the system need further increasing the temperature for reaction (e.g., 200 °C). Oppositely, an extremely high pressure of the system would be achieved if selecting a low temperature (e.g., <50 °C) to expand and then reaction at a high temperature. For example, expanding the solution at the tem-

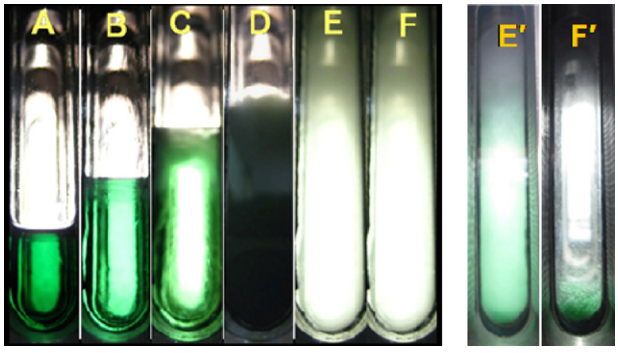

Fig. 2. Typical phase behavior of ethanol solution of $Ni(NO_3)_2$ (0.02 M) with CO_2 under stirring (A–E) at different pressures at 150 °C. (A) 0.1 MPa (ambient pressure), (B) 8 MPa, (C) 10 MPa, (D) 12 MPa, (E) 14.1 MPa, (F) the static phase of (E). (E′) Typical phase behavior of ethanol solution of $Ni(NO_3)_2$ (0.2 M) with CO_2-expansion (150 °C) at the pressure of 14.1 MPa, it is an inhomogeneous fluid even under stirring. (F′) the static phase of (E′).

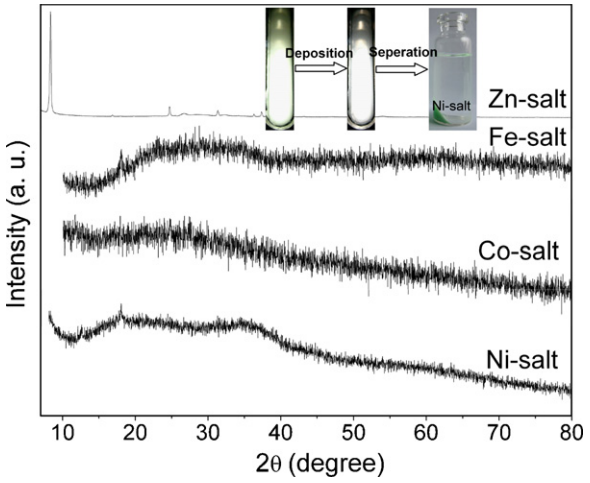

Fig. 3. XRD patterns of metal-salt synthesized in CO_2 expanded ethanol (conditions illustrated in Section 2). Inset shows the visual observations. The solid Ni-salt was obtained through centrifugation of the solution after reaction.

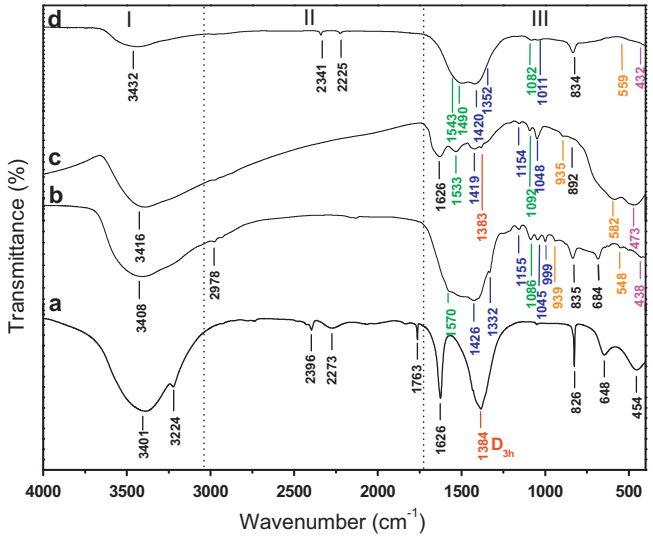

Fig. 4. FTIR spectra of primary precursor and metal-salts formed in CO_2 expanded ethanol. (a) $Ni(NO_3)_2{\cdot}6H_2O$. (b) Ni-salt. (c) Fe-salt. (d) Co-salt.

perature of 40 °C with a low pressure of 7.5 MPa and then increasing the temperature to 120 °C (at least for most precursors) for reaction directly result in a dangerous pressure that over 50 MPa.

Furthermore, it should be carefully to choose an appropriate concentration of hydrous inorganic metal salts because they have specific solubility in CO_2 expanded solution. Otherwise, it is impossible to form a homogeneous fluid, as shown in Fig. 2E′. An increased amount of primary green solution with un-dissolved precursors presented clearly on the bottom of autoclave if the concentration of $Ni(NO_3)_2{\cdot}6H_2O$ higher than 0.13 M (Fig. 2F′). Additionally, finely controlling the pumping rate of CO_2 (~7 ml/min) is also important when one introduces CO_2 to the system, overload always occur at high flowing rate due to the equilibrium delay.

3.2. Deposition mechanism of hydrous inorganic metal salt

At a relative low temperature, the homogeneous expanded fluid could be formed and stable for a long time without formation of any precipitates, and also it could return to pure ethanol solution after slowly releasing of CO_2. In most cases, enhancing temperature is required for the deposition of hydrous metal salts and the further in situ preparation of nanostructured materials. Generally, around temperatures of 150–200 °C the soluble hydrous metal salt could convert into a solid compound in CO_2 expanded ethanol, as observed from the indistinct viewable window (Fig. 3, inset picture). For a simple expression, an abbreviation of the solid compound was presented according to the element of metal, that is, metal-salt, Ni-salt for example, except for those identified ones. The XRD results (Fig. 3) show that most metal-salt have amorphous structure and that with a crystalline structure such as Zn-salt, it is difficult to find a standard materials because it is not a pure crystalline structure. The solid compounds have quite different FTIR spectrum compared to their precursors, such as Ni-salt and $Ni(NO_3)_2{\cdot}6H_2O$. As demonstrated in Fig. 4, the ionic compound of $Ni(NO_3)_2{\cdot}6H_2O$ has the characteristic absorption band at 1384 cm^{-1} ascribed to the asymmetric stretch band of free NO_3^- (D_{3h} symmetry) [29,30]. While for Ni-salt, the absorption band of free NO_3^- (1384 cm^{-1}) was disappeared and new absorption ones of M–OCO_2/(M–OCOO–) and M–ONO_2/(M–ONOO–) (C_{2v} symmetry) were emerged according to the results reported in the literature [31]. The new groups of CO_3^{2-} originated from the reactions of CO_2 and H_2O in this system. The interactions of metal ions with NO_3^- and CO_3^{2-} groups before and after reaction was proposed (Scheme 1) according to the spectrum information of FTIR in Fig. 4.

The bands labeled by green line was assigned to the antisymmetric stretching vibration of $\nu_4(-OCO_2)$ (1570–1490 cm^{-1}), the symmetric stretching vibration of $\nu_1(-OCO_2)$ (1155–1144 cm^{-1}) [32], and that labeled by blue line was assigned to the antisymmetric stretching vibration of $\nu_4(-ONO_2)$ (1485–1415 cm^{-1}), the symmetric stretching vibration of $\nu_1(-ONO_2)$ (1340–1305 cm^{-1}), the totally symmetric in-plane stretching vibration of $\nu_2(-ONO_2)$ (1087–1037 cm^{-1}) [29]. Furthermore, the absorption bands labeled in black line, including 825–895 cm^{-1} and 645–684 cm^{-1} were assigned, respectively, to the overlapped absorption band of the out-of-plane bending vibration of $\nu_6(-ONO_2)$ and $\nu_8(-OCO_2)$, the symmetric in-plane bending vibration of $\nu_3(-ONO_2)$ and $\nu_6(-OCO_2)$ [28–33]. The absorption band at 990–942 cm^{-1} and 540–582 cm^{-1} may be assigned to the vibration of ν(M–OH), (O–H...O) and (M–OH), respectively. The absorption band at 423–473 cm^{-1} may be assigned to the M–O stretching vibration [29,34]. Furthermore, the broad adsorption band at 3530–3400 cm^{-1} may be assigned to the stretching vibration ν(O–H...O)″ of the hydrogen bond [30], and that lower than 3400 cm^{-1} may be assigned to $\nu(H_2O)$. The investigation of the chemical bonds in the structure of the solid-compound offers a clear recognition on the conversion and the formation of the metal-salt from soluble metal salt to a solid one.

More directly, the presence of the element of C, H and N characterized by CHN-analysis strongly proved the existence of CO_3^{2-}, NO_3^- in the solid compound (Table 1). Interestingly, the content of C is higher than that of N, which demonstrates that the CO_3^{2-} originated from the CO_2 play an important role on the conversion of the precursors. Furthermore, a certain amount of water and the group of OH were also existed in the structure of metal-

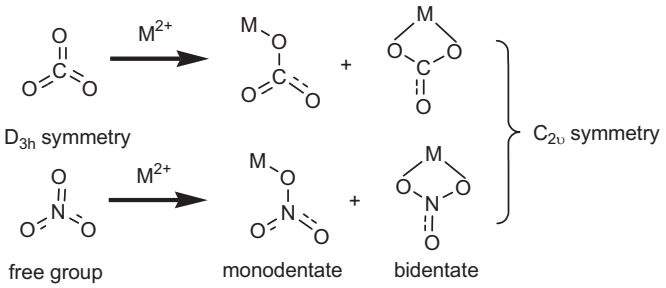

Scheme 1. Proposed interactions of metal ions with NO_3^- and CO_3^{2-} groups before and after reaction.

Table 1
The C, H, N content (wt.%) in metal-salt.

Metal-salt[a]	C	H	N
Ni-salt	12.4	3.04	3.06
Co-salt	12.74	1.99	3.99
Fe-salt	3.98	2.27	0.64

[a] Metal-salt is an abbreviation of $M_x(OH)_y(NO_3)_z(CO_3)_m{\cdot}nH_2O$ according to the element of metal, such as Ni-salt for $Ni_x(OH)_y(NO_3)_z(CO_3)_m{\cdot}nH_2O$.

salt because the process of dehydration and dehydroxylation were demonstrated clearly in the TGA measurement (Fig. 5). Therefore, the chemical formula of the solid compound could be expressed as $M_x(OH)_y(NO_3)_z(CO_3)_m{\cdot}nH_2O$ (M = any metals if only their ions have the ability of coordination). The value of *x*, *y*, *z*, *m* and *n* strongly depend on the experimental parameters, the kind and concentration of precursors, etc.

The chemical compositions of the metal-salt are quite different from the oxides formed in previous literature. In the past few years, a series of metal oxides (e.g., ZrO_2, Al_2O_3 and CeO_2) have been reported to form on CNTs through decomposition of the hydrous metal nitrates in the CO_2 expanded ethanol [24–26], and a proposition that the metal nitrates could decompose simply to oxides on the templates in CO_2 expanded ethanol was formed. Unfortunately, the reaction of metal nitrates was not as simple as illustrated, because they experience a more complex process with a coordination reaction and further decomposition process as confirmed later. Moreover, the template plays an essential role in affecting the chemical composition and crystalline structure of the precipitates, forming oxides on CNTs was only a specific example and the reason was largely ascribed to surface properties of CNTs [24–26].

To prove the result that the surface properties of the templates affect the deposition of hydrous inorganic metal salt, we further choose the carbon colloids and silica gel as the templates because their surface has a large amount of hydrophilic hydroxyl groups [27,28], which is opposite to the hydrophobic surface of CNTs [24–26]. Fig. 6 shows that varied solid compound was formed on the templates under the totally same conditions. For example, amorphous Zn-salt was always formed on surface of the carbon colloids, while crystalline $ZnCO_3$ (crystallite size, 20.4 nm) presented on the surface of SiO_2. More interestingly, the XRD patterns show crystalline Cu with a crystallite size of 32 nm was formed on the carbon colloids at a copper concentration of 0.01 M due to the reduction ability of hydroxyl groups (C–OH) on the surface of carbon colloids [27], while a new phase of Cu_2O presented and increased in the Cu phase with increasing the concentration of precursors gradually

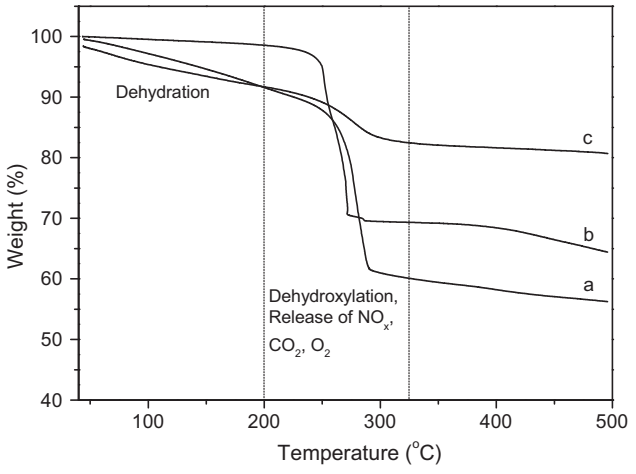

Fig. 5. Thermogravimetric Analysis curves of synthesized metal-salts. (a) Ni-salt, (b) Co-salt, (c) Fe-salt.

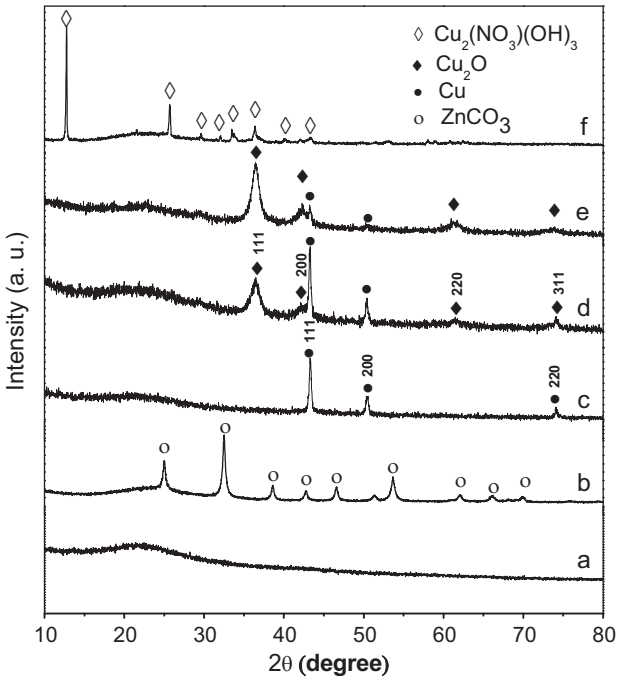

Fig. 6. XRD patterns of the metal-salts formed on carbon colloids and silica nanoparticles. (a) Zn-salt/C (0.03 M). (b) $ZnCO_3/SiO_2$ (0.02 M). (c) Cu/C (0.01 M). (d) $Cu–Cu_2O/C$ (0.02 M). (e) $Cu_2O–Cu/C$(0.03 M). (f) $Cu_2(NO_3)(OH)_3/SiO_2$ (0.02 M).

(Fig. 6), this should be ascribed to the limited amount of the reductant C–OH which was not enough to reduce the increased amount of Cu_2O. While changing the template to SiO_2 gel, $Cu_2(NO_3)(OH)_3$ was formed, irrespective to the concentration of precursors. Obviously, the basic property of hydroxyl groups on silica gel as well as its hydrophilicity largely affects the chemical compositions and crystallite size (e.g., 81.7 nm at a concentration of 0.02 M). Undoubtedly, the surface properties of templates play a decisive role in the deposition of hydrous metal salt. While in most cases, amorphous $M_x(OH)_y(NO_3)_z(CO_3)_m{\cdot}nH_2O$ (M = Ni, Fe, Co, Cr, etc.) were always formed on the carbon colloids and silica gel, as illustrated in the absence of templates in CO_2 expanded ethanol.

Base on the above analysis, a coordination–decomposition (C–D) deposition mechanism was proposed in CO_2 expanded ethanol. Firstly, the hydrous inorganic metal salt was dissociated in ethanol to form a solution consisting of M^{2+}, NO_3^{2-}, H_2O. With the introduction of CO_2, the H_2O reacted with CO_2 to generate the ions of CO_3^{2-} and HCO_3^-. Before the deposition, the free groups of NO_3^{2-} and CO_3^{2-} (D_{3h} symmetry) interact with M^{2+} through electronic interaction in the expanded homogeneous fluid (Fig. 7A). At the temperature of reaction, the dissociated anions such as NO_3^- and CO_3^{2-}, together with molecules (H_2O), could coordinate directly to the matrix M^{2+} by bridged oxygen to form a solid-compound (Fig. 7A and B). Due to the strength of the coordinate bond higher than electronic bond, the compound could be formed stably and precipitated from the fluid. Herein, it is clear that the formation of metal oxide was resulted from the decomposition of such solid-compounds rather than a simple "decomposition" from the primary precursors as reported before [24–26]. Therefore the C–D deposition mechanism seems more rational to demonstrate the reaction behaviors of precursors and further interpret the reason of the formation of oxides when CNTs were used in similar system. Furthermore, based on the knowledge of our C–D mechanism, the precursors could be extended to chlorides except those limited nitrates because the group of CO_3^{2-} resulted from CO_2 has a strong coordination ability with metallic ions, even the coordination ability of Cl^- is weak. Consequently, the C–D mechanism could also

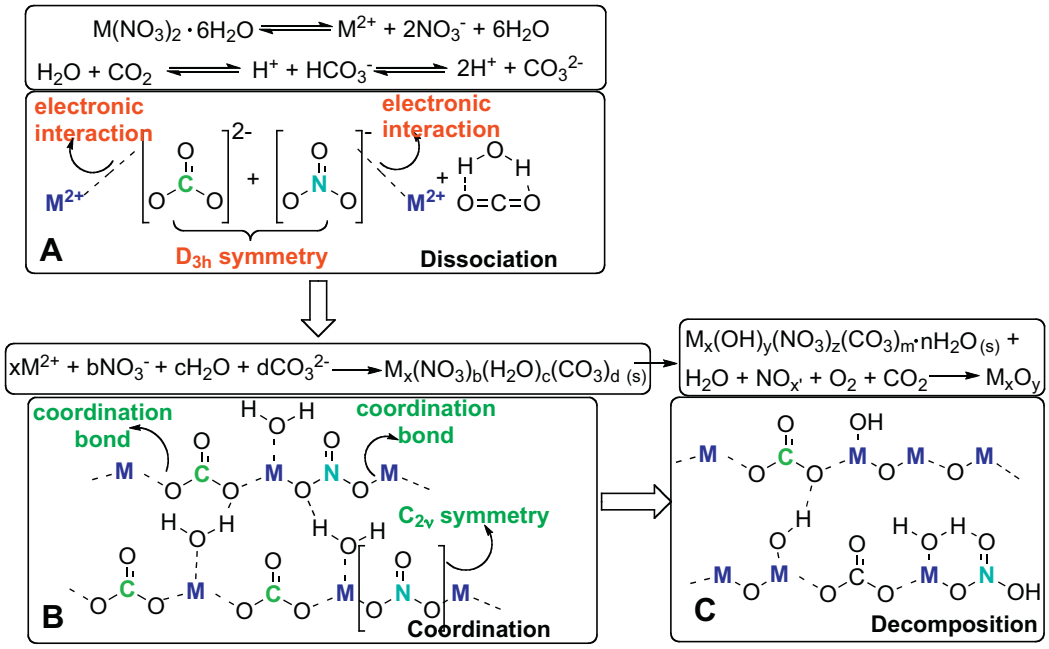

Fig. 7. Proposed deposition mechanism (C–D) of hydrous inorganic metal salt (e.g., metal nitrates) in $scCO_2$ expanded ethanol. (A) Behavior of dissociated ions and molecules. Right inset is the expanded ethanol solution of $Co(NO_3)_2{\cdot}6H_2O$. (B) Coordination of ions and molecules to form a solid-compound, right inset is the clear expanded fluid after coordination. (C) Further decomposition of the solid-compound.

Table 2
Concentration of metal ions determined by inductively coupled plasma atomic emission spectrometer (ICP-AES) analysis.

Cations	Anions	Initial concentration (C_0/mmol L^{-1})	Residual concentration (C_r/mmol L^{-1})[a]	The percentage of coordination (%)
Ni^{2+}	NO_3^-	20	0.11	99.45
Co^{2+}	NO_3^-	10	0.05	99.50
Cr^{2+}	NO_3^-	15	0.05	99.67
Zn^{2+}	NO_3^-	20	0.04	99.80
Nd^{3+}	NO_3^-	20	0.03	99.85
Cu^{2+}	NO_3^-	30	0.04	99.87
Fe^{2+}	NO_3^-	20	0.01	99.95
Sn^{2+}	Cl^-	20	4.12	79.40
Mn^{2+}	Cl^-	20	1.30	93.50
Pd^{2+}	Cl^-	1	0	100

[a] C_r is the concentration of cations remained in ethanol solution after reaction.

well interpret the reason of the formation of oxides from metal chlorides, such as $SnCl_2{\cdot}4H_2O$ [35].

3.3. Coordination ability of metal ions in CO_2 expanded solution

Except the knowledge of the deposition mechanism, the coordinating ability of metal ions in CO_2 expanded ethanol as well as the deposition rates of hydrous metal salts were discussed systematically. The generation of the solid compounds and the changing color of the solution were observed for determining the starting and ending of the deposition reactions (Fig. 7A–C). Preliminary results of observations showed that the reaction rate sequence of nitrites was Fe (2 min) ≫ Cu (10 min) > Zn (14 min) ~ Cr (15 min) > Co (30 min) > Ni (50 min), which may correlate with the hydrolysis reaction rate of these metal ions. Furthermore, almost all the precursors could be converted into metal-salt within 2 h because the percentage of coordinated metal ions ($(C_0 - C_r)/C_0$; C_0 = primary concentration of precursors; C_r = residual precursors) was always higher than 99%, as determined by the results of ICP-AES (Table 2). Meanwhile, metal chlorides, such as $SnCl_2{\cdot}4H_2O$ and $MnCl_2{\cdot}4H_2O$, could also be converted into solid compounds with high conversion of 79.4% and 93.5%, respectively, which strongly confirmed our presented C–D mechanism that CO_3^{2-} could coordinate with M^{2+} even for the chlorides with a weak coordination ability of Cl^- groups. Moreover, the other element such as rare earth (e.g., Nd^{3+}, 99.83% conversion) and noble metal salt (e.g., Pd^{2+}, 99.97% conversion) could be completely converted into solid compounds. Obviously, the CO_2 expanded ethanol was an effective medium to convert the soluble hydrous metal salt into a solid compound; thereby this method could be extensively adopted in the fabrication of nanostructured materials, especially for those are difficult to prepare in traditional solvents.

4. Conclusions

In this contribution, we presented a fundamental study of the deposition reaction mechanism of hydrous inorganic metal salts in CO_2 expanded ethanol. The reaction behavior of precursors in CO_2 expanded ethanol, including phase behavior, deposition mechanism, coordination ability and rates of precursors have been discussed in detail. A coordination–decomposition (C–D) mechanism of hydrous inorganic metal salt was proposed for the first time. It shows the probable conversion of every kind chemical group from dissociated ions to form a solid compound in CO_2 expanded ethanol. Furthermore, the effects of the templates and the roles of CO_2 and H_2O during the deposition of precursors were also studied. With the recognition of the whole process and detailed mechanism, the fabrication of nanostructured materials with the deposition of varied

metal-salts on a wide range of templates such as fibers, particles, porous silica and carbon becomes more directly and clearly.

Acknowledgment

This work was financially supported by the One Hundred Talent Program of CAS, NSFC 20873139, and KJCX2, YWH16.

References

[1] J.J. Watkins, T.J. Mccarthy, Polymer/metal nanocomposite synthesis in supercritical CO_2, Chemistry of Materials 7 (1995) 1991–1994.
[2] S. Haji, Y. Zhang, C. Erkey, Atmospheric hydrodesulfurization of diesel fuel using Pt/Al_2O_3 catalysts prepared by supercritical deposition for fuel cell applications, Applied Catalysis A: General 374 (2010) 1–10.
[3] Y. Zhang, C. Erkey, Preparation of platinum–Nafion–carbon black nanocomposites via a supercritical fluid route as electrocatalysts for proton exchange membrane fuel cells, Industrial & Engineering Chemistry Research 44 (2005) 5312–5317.
[4] B. Cangul, L.C. Zhang, M. Aindow, C. Erkey, Preparation of carbon black supported Pd, Pt and Pd–Pt nanoparticles using supercritical CO_2 deposition, J. Supercritical Fluids 50 (2009) 82–90.
[5] J.M. Blackburn, D.P. Long, J.J. Watkins, Reactive deposition of conformal palladium films from supercritical carbon dioxide solution, Chemistry of Materials 12 (2000) 2625–2631.
[6] N.E. Fernandes, S.M. Fisher, J.C. Poshusta, D.G. Vlachos, M. Tsapatsis, J.J. Watkins, Reactive deposition of metal thin films within porous supports from supercritical fluids, Chemistry of Materials 13 (2001) 2023–2031.
[7] J.M. Blackburn, D.P. Long, A. Cabanas, J.J. Watkins, Deposition of conformal copper and nickel films from supercritical carbon dioxide, Science 294 (2001) 141–145.
[8] A. Cabanas, X.Y. Shan, J.J. Watkins, Alcohol-assisted deposition of copper films from supercritical carbon dioxide, Chemistry of Materials 15 (2003) 2910–2916.
[9] Y.F. Zong, J.J. Watkins, Deposition of copper by the H_2-assisted reduction of Cu(tmod)(2) in supercritical carbon dioxide: kinetics and reaction mechanism, Chemistry of Materials 17 (2005) 560–565.
[10] Y. Zhang, D.F. Kang, M. Aindow, C. Erkey, Preparation and characterization of ruthenium/carbon aerogel nanocomposites via a supercritical fluid route, J. Physical Chemistry B 109 (2005) 2617–2624.
[11] C.F. Karanikas, J.J. Watkins, Kinetics of the ruthenium thin film deposition from supercritical carbon dioxide by the hydrogen reduction of Ru(tmhd)(2)cod, Microelectronic Engineering 87 (2010) 566–572.
[12] T. Hasell, L. Lagonigro, A.C. Peacock, S. Yoda, P.D. Brown, P.J.A. Sazio, S.M. Howdle, Silver nanoparticle impregnated polycarbonate substrates for surface enhanced Raman spectroscopy, Advanced Functional Materials 18 (2008) 1265–1271.
[13] B. Wong, S. Yoda, S.M. Howdle, The preparation of gold nanoparticle composites using supercritical carbon dioxide, J. Supercritical Fluids 42 (2007) 282–287.
[14] C. Erkey, Preparation of metallic supported nanoparticles and films using supercritical fluid deposition, J. Supercritical Fluids 47 (2009) 517–522.
[15] A.H. Romang, J.J. Watkins, Supercritical fluids for the fabrication of semiconductor devices: emerging or missed opportunities? Chemical Reviews 110 (2010) 459–478.
[16] R.H. Sui, S.Y. Liu, G.A. Lajoie, P.A. Charpentier, Preparing titania aerogel monolithic chromatography columns using supercritical carbon dioxide, J. Separation Science 33 (2010) 1604–1609.
[17] R.H. Sui, A.S. Rizkalla, P.A. Charpentier, Formation of titania nanofibers: a direct sol–gel route in supercritical CO_2, Langmuir 21 (2005) 6150–6153.
[18] R.A. Lucky, P.A. Charpentier, N-doped ZrO_2/TiO_2 bimetallic materials synthesized in supercritical CO_2: morphology and photocatalytic activity, Applied Catalysis B: Environmental 96 (2010) 516–523.
[19] N. Tatsuda, H. Itahara, N. Setoyama, Y. Fukushima, Preparation of titanium dioxide in the nano-spaces of activated carbon using carbon dioxide supercritical fluid as a solvent, J. Materials Chemistry 14 (2004) 3440–3443.
[20] H. Wakayama, H. Itahara, N. Tatsuda, S. Inagaki, Y. Fukushima, Nanoporous metal oxides synthesized by the nanoscale casting process using supercritical fluids, Chemistry of Materials 13 (2001) 2392–2396.
[21] A. O'Neil, J.J. Watkins, Reactive deposition of conformal metal oxide films from supercritical carbon dioxide, Chemistry of Materials 19 (2007) 5460–5466.
[22] Y. Wang, Z.M. Liu, B.X. Han, Z.Y. Sun, J.M. Du, J.L. Zhang, T. Jiang, W.Z. Wu, Z.J. Miao, Replication of biological organizations through a supercritical fluid route, Chemical Communications (2005) 2948–2950.
[23] O. Aschenbrenner, S. Kemper, N. Dahmen, K. Schaber, E. Dinjus, Solubility of beta-diketonates, cyclopentadienyls, and cyclooctadiene complexes with various metals in supercritical carbon dioxide, J. Supercritical Fluids 41 (2007) 179–186.
[24] L. Fu, Y.Q. Liu, Z.M. Liu, B.X. Han, L.C. Cao, D.C. Wei, G. Yu, D.B. Zhu, Carbon nanotubes coated with alumina as gate dielectrics of field-effect transistors, Advanced Materials 18 (2006) 181–185.
[25] Z.Y. Sun, X.R. Zhang, B.X. Han, Y.Y. Wu, G.M. An, Z.M. Liu, S.D. Miao, Z.J. Miao, Coating carbon nanotubes with metal oxides in a supercritical carbon dioxide–ethanol solution, Carbon 45 (2007) 2589–2596.
[26] Z.Y. Sun, X.R. Zhang, N. Na, Z.M. Liu, B.X. Han, G.M. An, Synthesis of ZrO2–carbon nanotube composites and their application as chemiluminescent sensor material for ethanol, J. Physical Chemistry B 110 (2006) 13410–13414.
[27] X.M. Sun, Y.D. Li, Colloidal carbon spheres and their core/shell structures with noble-metal nanoparticles, Angewandte Chemie-International Edition 43 (2004) 597–601.
[28] W. Stober, A. Fink, E. Bohn, Controlled growth of monodisperse silica spheres in micron size range, J. Colloid and Interface Science 26 (1968) 62–69.
[29] K. Petrov, N. Zotov, E. Mirtcheva, O. Garciamartinez, R.M. Rojas, Effect of composition on the lattice-parameters and thermal-behavior of nickel(II)–cobalt(II) hydroxide nitrate solid–solutions, J. Materials Chemistry 4 (1994) 611–614.
[30] N. Zotov, K. Petrov, M. Dimitrovapankova, Infrared-spectra of Cu(II)–Co(II) mixed hydroxide nitrates, J. Physics and Chemistry of Solids 51 (1990) 1199–1205.
[31] W. Gu, C.P. Tripp, Reaction of silanes in supercritical CO_2 with TiO_2 and Al_2O_3, Langmuir 22 (2006) 5748–5752.
[32] J. Fujita, A.E. Martell, K. Nakamoto, Infrared spectra of metal chelate compounds. 8. Infrared spectra of Co(III) carbonato complexes, J. Chemical Physics 36 (1962) 339–345.
[33] C.C. Addison, B.M. Gatehouse, The infrared spectra of anhydrous transition-metal nitrates, J. Chemical Society (1960) 613–616.
[34] Z.P. Xu, H.C. Zeng, Abrupt structural transformation in hydrotalcite-like compounds $Mg_{1-x}Al_x(OH)_2(NO_3)_x \cdot nH_2O$ as a continuous function of nitrate anions, J. Physical Chemistry B 105 (2001) 1743–1749.
[35] Z.Y. Sun, Z.M. Liu, B.X. Han, G.M. An, Supercritical carbon dioxide-assisted deposition of tin oxide on carbon nanotubes, Materials Letters 61 (2007) 4565–4568.